


WEG1, which encodes a cell wall hydroxyproline-rich glycoprotein, is essential for parental root elongation controlling lateral root formation in rice

Nonawin Lucob-Agustin^a, Tsubasa Kawai^a, Misuzu Takahashi-Nosaka^b, Mana Kano-Nakata^c, Cornelius M. Wainaina^d, Tomomi Hasegawa^a, Mayuko Inari-Ikeda^c, Moeko Sato^e, Hiroyuki Tsuji^e, Akira Yamauchi^a and Yoshiaki Inukai^{c,f,*} 

^aGraduate School of Bioagricultural Sciences, Nagoya University, Nagoya, Aichi, 464-8601, Japan

^bDepartment of Genomics and Evolutionary Biology, National Institute of Genetics, Mishima, Shizuoka, 411-8540, Japan

^cInternational Center for Research and Education in Agriculture, Nagoya University, Nagoya, Aichi, 464-8601, Japan

^dDepartment of Horticulture, Jomo Kenyatta University of Agriculture and Technology, Nairobi, Kenya

^eKihara Institute for Biological Research, Yokohama City University, Yokohama, Kanagawa, 244-0813, Japan

^fPREST, JST, Kawaguchi, Saitama, 332-0012, Japan

Correspondence

*Corresponding author,

e-mail: inukaiy@agr.nagoya-u.ac.jp

Received 18 September 2019;

revised 18 December 2019

doi:10.1111/ppl.13063

Lateral roots (LRs) determine the overall root system architecture, thus enabling plants to efficiently explore their underground environment for water and nutrients. However, the mechanisms regulating LR development are poorly understood in monocotyledonous plants. We characterized a rice mutant, *wavy root elongation growth 1* (*weg1*), that produced higher number of long and thick LRs (L-type LRs) formed from the curvatures of its wavy parental roots caused by asymmetric cell growth in the elongation zone. Consistent with this phenotype, was the expression of the *WEG1* gene, which encodes a putative member of the hydroxyproline-rich glycoprotein family that regulates cell wall extensibility, in the root elongation zone. The asymmetric elongation growth in roots is well known to be regulated by auxin, but we found that the distribution of auxin at the apical region of the mutant and the wild-type roots was symmetric suggesting that the wavy root phenotype in rice is independent of auxin. However, the accumulation of auxin at the convex side of the curvatures, the site of L-type LR formation, suggested that auxin likely induced the formation of L-type LRs. This was supported by the need of a high amount of exogenous auxin to induce the formation of L-type LRs. These results suggest that the MNU-induced *weg1* mutated gene regulates the auxin-independent parental root elongation that controls the number of likely auxin-induced L-type LRs, thus reflecting its importance in improving rice root architecture.

Introduction

The fibrous root system of rice, similar to other cereal crops, is comprised of a seminal root and numerous crown roots and their lateral roots (LRs) whose overall growth and angle determine the root system architecture (Rebouillat

et al. 2009, Uga et al. 2015). Furthermore, LRs have been categorized into distinct types substantially varying in length, diameter and histological structures (Kono et al. 1972). The S-type LRs are short with no branches and have a thin diameter and simple vasculature, but are normally

Abbreviations – FAA, formaldehyde acetic acid; GUS, β -glucuronidase; HRGP, hydroxyproline-rich glycoprotein; IAA, indole-3 acetic acid; LRs, lateral roots; *weg1*, *wavy root elongation growth 1*.

numerous, whereas the L-type LRs are generally long, have a thick diameter and well-developed vasculature, and are highly branched (Yamauchi et al. 1996, Wang et al. 2005). In addition, they have different genetic controls (Niones et al. 2015, Suralta et al. 2015).

Because the total root length of the whole root system is composed of LRs (Yamauchi et al. 1987), the frequency and branching of L-type LRs is important to extend the entire root system for absorbing water and nutrients into a larger soil volume. This has profound implications in enhancing productivity (shoot dry matter production and yield) under abiotic stresses such as drought or soil moisture fluctuations (reviewed by Suralta et al. 2016) or suboptimal soil conditions (Lynch 2007), which become increasingly challenging over time because of the recent climate change (IPCC 2014). Understanding the genetic control of the LR trait and its mechanisms, therefore, holds potential in the manipulation and improvement of the root system architectural traits to enhance both productivity and climate resilience of rice plants. In this regard, we found and analyzed a rice recessive mutant, designated as *wavy root elongation growth 1* (*weg1*), which exhibits a high number of L-type LRs arising from the convex side of the wavy pattern of parental roots.

Several mutants showing wavy, bending and skewed roots have been identified and characterized in *Arabidopsis thaliana* that have contributed to our understanding of the mechanisms regulating such phenotype (Mochizuki et al. 2005, Ditengou et al. 2008, Oliva and Dunand 2007). To date, gravitropism, the mechanism by which plant organs use gravity as a directional cue for growth, has received the utmost attention (reviewed in Masson 1995, Blancaflor and Masson 2003). The deviation of growth from the gravitational field results in differential cell growth because of asymmetric auxin distribution across the root that occurs when the movement of auxin to the elongation zone is higher on one side than on the other (Kleine-Vehn et al. 2010, Barbez et al. 2017). In rice, the asymmetric distribution of auxin similarly regulates the gravitropic root response. The quantitative trait locus *DEEPER ROOTING 1* that controls cell elongation, causing root gravitropic bending, was found to be regulated by asymmetric auxin distribution (Uga et al. 2011, 2013). In addition, *villin2* (Wu et al. 2015) and *Ospin2* (Inahashi et al. 2018) were reported to exhibit wavy/twisted parental root elongation via the action of auxin. However, these mutants did not produce developed LRs along their curvatures. The relationship between LR development and parental root bending has not been studied thus far.

In this study, we present a MNU-induced *weg1* rice mutant that displayed a wavy root phenotype in which

the curvature is the site of LR organ formation. We demonstrate that *WEG1* is a putative member of the cell wall hydroxyproline-rich glycoprotein (HRGP) family, and the *weg1* mutated gene regulates the auxin-independent parental root elongation that controls the number of L-type LRs likely induced by auxin.

Materials and methods

Plant materials and growth conditions

The *weg1* mutant was obtained by mutagenizing *Oryza sativa* cv. Taichung65 with *N*-methyl-*N*-nitrosourea (MNU) as described by Inahashi et al. (2018). Briefly, the panicle-dipping method (Satoh and Omura 1979) was employed to treat fertilized egg cells of rice plants with MNU. The treated panicles were harvested approximately 40 days after the treatment to obtain the M_1 seeds, which were subsequently grown in a paddy field to get the M_2 seeds. Subsequently, the mutants were screened by evaluating the root phenotypes of 2-week-old M_2 seedlings.

The seeds of the wild-type, *weg1* mutants and F_2 plants derived from the crosses between the mutants and *O. sativa* cv. Kasalath were pregerminated using water mixed with fungicide (benomyl benlate, 0.15% w/v) and incubated in a chamber (LH-241SP, Biotron) 72 h prior to transferring them into a non-aerated 9 l black box with $1/10$ strength nutrient solution as described by Colmer (2003) for 2 weeks. The growth chamber had the following conditions: 28°C, 75% humidity and $350 \mu\text{mol m}^{-2} \text{s}^{-1}$ light intensity at a continuous light.

For phenotyping, seedlings of the wild-type, *weg1* mutant and double mutant between *weg1* and *Osiaa13* (Inahashi et al. 2018) were grown for 2 weeks in the same growth conditions as mentioned above.

For exogenous auxin treatment using indole-3 acetic acid (IAA), wild-type seedlings were grown vertically in tap water for 10 days in the same chamber condition mentioned above.

Transgenic plants were routinely grown on MS medium (Murashige and Skoog 1962) containing 3% (w/v) sucrose and 0.3% Gelrite.

Map-based cloning, plasmid constructs and plant transformation

To map the causative gene of the mutants, a linkage analysis was performed using F_2 plants derived from a cross between the *weg1* mutant (derived from 'Taichung65', *japonica* variety) and wild-type Kasalath (*indica* variety). For the complementation of the *weg1* mutation, the wild-type genomic sequence of 'Taichung65' was amplified in the region extending from approximately -3 kbp to +7 kbp (considering the *WEG1* translation site as

+1 bp) and was cloned into the pHGW vector to generate the *ProWEG1:WEG1* construct. For generating the *DR5:NSL-3xVenus* construct, we first prepared the plasmid vector pENTR DR5-NLS-3xVenus by linking the DR5rev promoter sequence with a fusion gene encoding the nuclear localization signal and tandem triplicate of the fluorescent protein Venus. The *DR5:NSL-3xVenus* fragment was then transferred from pENTR into pGWB501 (Nakagawa et al. 2007) using the Gateway LR reaction.

For constructing *ProWEG1:GUS*, the genomic sequence of *WEG1* from approximately -3 kbp to -1 bp and the β -glucuronidase (*GUS*) sequence with the nopaline synthase polyadenylation signal (*nos*) terminator in the pGWB3 vector (Nakagawa et al. 2007) were amplified. The resulting PCR products were fused and cloned into the *Xba*I and *Hind*III sites of the pCAM-BIA1300 vector.

The resulting fusion constructs were introduced into *Agrobacterium tumefaciens* strain EHA105 by electroporation. The *Agrobacterium*-mediated transformation of rice was then performed as described previously (Hiei et al. 1994, Ozawa 2009). Transgenic plants were selected on MS medium containing 50 mg l⁻¹ hygromycin at 30°C.

Morphological characterization

The lengths of the seminal root, crown roots and shoot of 2-week-old seedlings were measured manually using a ruler. The number of LRs on the seminal root and gravistimulated root was counted and classified into two distinct types, S-type and L-type LRs, using a microscope. The S-type LRs are short with a thin diameter, and non-branching, but normally numerous, whereas the L-type LRs are generally long with a thick diameter and higher-order of LR branching (Yamauchi et al. 1996, Wang et al. 2005, Kawai et al. 2017). Although the crown roots and L-type LRs also produce S-type LRs, we only counted the number of LRs along the seminal root in the present study. Gravistimulation of wild-type root was performed using 2-day-old wild-type roots grown vertically under the same nutrient condition. After transfer of the roots into 1% agar, the root was rotated from the vertical to horizontal at 90°.

To further examine the growth pattern of the mutant at maturity, a set of seedlings was grown under field conditions. The plant height and panicle number were recorded upon harvest.

Histological analysis

To check the cell division rate, the Click-iTTM EdU Alexa Fluor[®] Imaging Kit (Invitrogen/Molecular Probes) was

used according to the described protocol with modifications. Firstly, the 4-day-old seedling roots were exposed to 1 l of water supplemented with 0.01 g EdU and 1 ml DMSO for 4 h in chamber conditions. After staining, the root samples were fixed in FAA (formaldehyde: acetic acid:50% ethanol at 1:1:18) solution and permeabilized with the Triton solution. Thereafter, azides were incorporated coupled with Alexa Fluor 488. Upon the completion of the EdU Click-iT reaction, the samples were washed first in graded ethanol series, then in salicylic acid: ethanol series (2:1, 1:1, 1:2), and finally in 100% salicylic acid for transparency. The samples were mounted, and the images of the cleared seminal roots were captured using a laser scanning microscope (FV1000; Olympus). The images of the Alexa Fluor 488-labeled root samples were captured using an excitation wavelength of 488 nm, and the signal was detected at a wavelength of 510–530 nm, while the autofluorescence of the root samples was captured using an excitation wavelength of 405 nm, and the signal was detected at 450–470 nm.

For measuring cell length, 2-cm root tip segments of the wild-type and *weg1* mutant plants were fixed in FAA for 24 h at 4°C and then dehydrated in a graded ethanol series. Subsequently, the samples were treated with salicylic acid for transparency and viewed under a laser scanning microscope (FV1000; Olympus).

For the observations of the expression of *DR5:NSL-3xVenus* in wild-type and mutant, 2-cm sections from the root tip and curve regions were sampled and directly viewed under a laser scanning microscope (FV1000; Olympus). The images of the root samples were captured using an excitation wavelength of 488 nm, and the signal was detected at a wavelength of 510–530 nm, while the autofluorescence of the root samples was captured using an excitation wavelength of 405 nm, and the signal was detected at 450–470 nm.

Expression analysis

Total RNA was extracted from the different zones of the seminal roots of wild-type and mutant seedlings using the NucleoSpin[®] RNA Plant Kit (Macherey-Nagel) according to the manufacturer's instructions. The RNA quantity was determined by measuring the optical density at 260 nm, and 25 ng total RNA was used as template to measure the transcript levels. A quantitative real-time PCR (qRT-PCR) was performed using the One-Step SYBR PrimeScript RT-PCR Kit II (Perfect Real Time) (TaKaRa Bio) and StepOnePlus Real-Time PCR (Life Technologies). The expression level of the *WEG1* gene was normalized to the expression level of *Ubiquitin* as internal

control. The primer sequences used for the qRT-PCR are shown in Table S1.

The expression of the GUS protein was detected by staining the samples in GUS buffer (1 mM X-Gluc, 50 mM Na-P buffer [pH 7.0], 70% methanol, and 0.1% Triton X-100) overnight. The stained samples were destained in ethanol until the chlorophyll was bleached and, thereafter, were observed under a stereomicroscope (SZX16; Olympus).

Data analysis

The inheritance mode of the mutant's phenotypic traits was examined by determining the segregation ratio of the phenotype in each M_3 progeny using the Chi-square test. The shoot and root characteristics, *WEG1* expression level in the roots, and effects of IAA were compared using a Student's *t*-test or analysis of variance (ANOVA) and a multiple-comparison Tukey's test in R commander version 3.5.1. (Fox 2005).

Results

Identification and phenotypic characterization of the *weg1* mutant

To investigate the molecular mechanisms controlling root architecture in rice, we screened a mutant line with altered root morphology from the M_2 population of *O. sativa* 'Taichung65' mutagenized with *N*-methyl-*N*-nitrosourea (MNU) and grown under nutrient culture conditions. One of the mutants displayed wavy parental roots, including the seminal and crown roots, with a high number of developed L-type LR, which are long, thick in diameter and capable of branching, arising from the convex side of the curvatures (mean number of curvatures on the basis of 0–10 cm seminal root axis \pm SE: 4.86 ± 0.64) as compared to the wild-type plants (0.35 ± 0.17), which displayed straight parental root growth (Fig. 1A–C, I). This mutant line was designated as *weg1*. Other component root traits of the mutant, such as seminal root length and crown root number (Fig. 1E, F), were similar to the

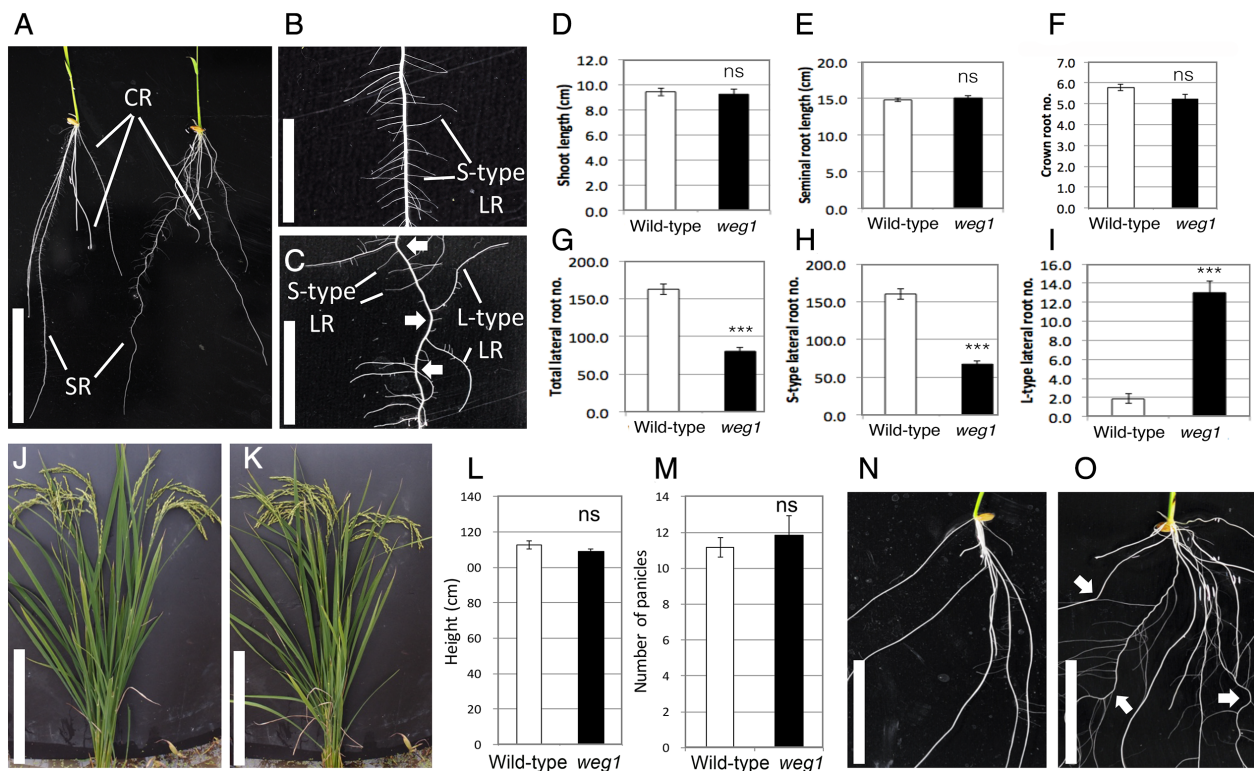


Fig. 1. Phenotypic characterization of *weg1* mutant. (A) Root phenotype of the wild-type (left) and *weg1* mutant (right) at 2 weeks after germination. SR, seminal root; CR, crown root. Scale bar = 2.5 cm. (B, C) Close-up of the parental roots and lateral roots in wild-type (B) and *weg1* (C) mutant. LR, lateral root, arrow indicates curvature. Scale bar = 1 cm. (D–I) Shoot and root traits measured at seedling stage. Values represent means \pm SE ($n = 8$) (J, K) Mature plant aerial phenotypes of field-grown wild-type and *weg1* mutant, respectively. Scale bar = 2 cm. (L, M) Plant height and panicle number measured at maturity, respectively. Values represent means \pm SE ($n = 6$). (N, O) Root phenotypes of 2-week-old *Osiaa13* (N) and *weg1 Osiaa13* mutants (O). Arrows point to the curvatures. Scale bar = 20 cm. Statistical significance at $***P < 0.001$ between genotypes was revealed by two-tailed Student's *t*-test (ns, non-significant).

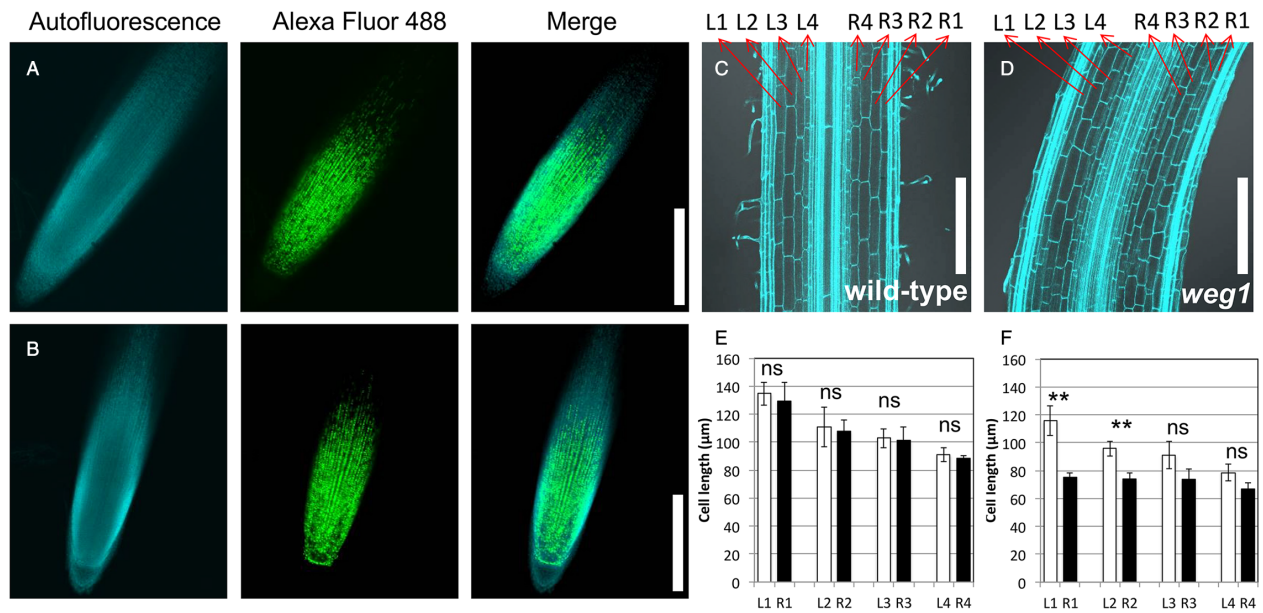


Fig. 2. Comparison of the cell division rate and cell elongation in wild-type and *weg1* mutant roots. (A, B) Dividing cells in the root apical meristem, represented by green color, of 4-day-old wild-type (above photos) and *weg1* mutant (below photos) grown under $1/10$ nutrient solution. Scale bars = 300 μm. (C, D) Cell lengths of the straight region in the elongation zone of the wild-type (C) and the corresponding region of mutant (D) that is curved. Arrows show the indicated cortical cell layers measured. L and R, left and right sides, respectively. 1–4 indicates the cortical cell layers from the outermost to innermost side. Scale bar = 100 μm. (E, F) Comparison of the cortical cell length between left and right sides from the outermost to innermost cortical cell layers between wild-type and mutant, respectively. Values represent means \pm SE (n = 5). Statistical significance at $**P < 0.01$ in the means between genotypes was revealed by two-tailed Student's *t*-test (ns, non-significant).

wild-type plant. However, compared to the wild-type root, the mutant root had a lower total number of LRs, but that was because it had fewer S-type LRs, which are short and thin in diameter. (Fig. 1G, H). Despite the wavy root phenotype, the shoot length of the mutant plant was also similar to that of the wild-type plant (Fig. 1D).

To analyze the shoot growth pattern of the mutant up to the maturity stage, we grew the *weg1* mutant under field conditions and observed that its aerial parts appeared normal and could grow vigorously (Fig. 1J, K). The plant height and panicle number of the mutant plant were comparable to the wild-type plant (Fig. 1L, M).

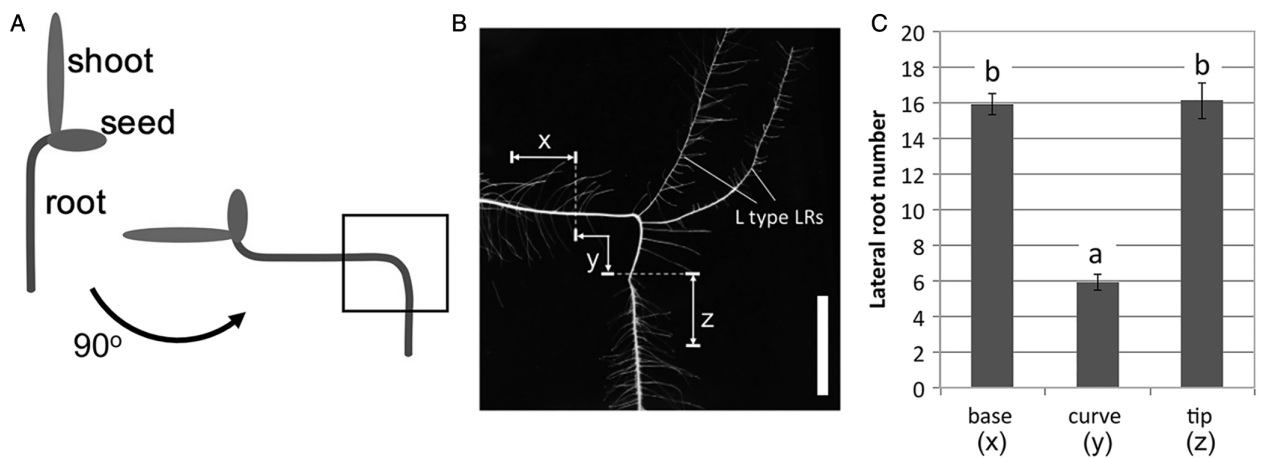


Fig. 3. Effects of bending on lateral root development. (A, B) Gravistimulation of 2-day-old wild-type root (grown on the surface of 1% agar) by rotation from vertical to horizontal at 90°. (B) Regions of the bent roots in the seminal root counted for the number of lateral roots after 2 weeks of growth: x, base region; y, curve; z, tip region. Scale bar = 0.5 cm. (C) The number of lateral roots at each measured regions of the bent roots. Values represent means \pm SE (n = 10). Different lowercase letters denote significant differences among regions ($P < 0.05$, 1-way ANOVA followed by Tukey's test for multiple comparisons).

Histological characterizations of the cell elongation pattern in the mutant

Previous studies reported that wavy root is primarily caused by differential growth at opposite root flanks (Buer et al. 2003, Oliva and Dunand 2007). To understand the cellular basis of the wavy root phenotype, we performed histological analyses on the root tip of the vertically grown *weg1* mutant and wild-type seedlings. We examined the cell division pattern by applying EdU to the root apical meristem of the mutant and wild-type plants. We did not find

any significant difference in the EdU-covered (dividing) cells in the division zone (Fig. 2A, B). On the other hand, the cells in the elongation zone exhibited differential growth in the *weg1* mutant roots (Fig. 2C, D), wherein the cell lengths at the convex (outer) side of the mutant were significantly longer than those at its concave (inner) side (Fig. 2F) as revealed by the transparent images. The asymmetric cell length was mainly due to the reduction of the lengths of the cortical cells at the concave side. However, no difference in cell length was observed on either side of the wild-type roots (Fig. 2E).

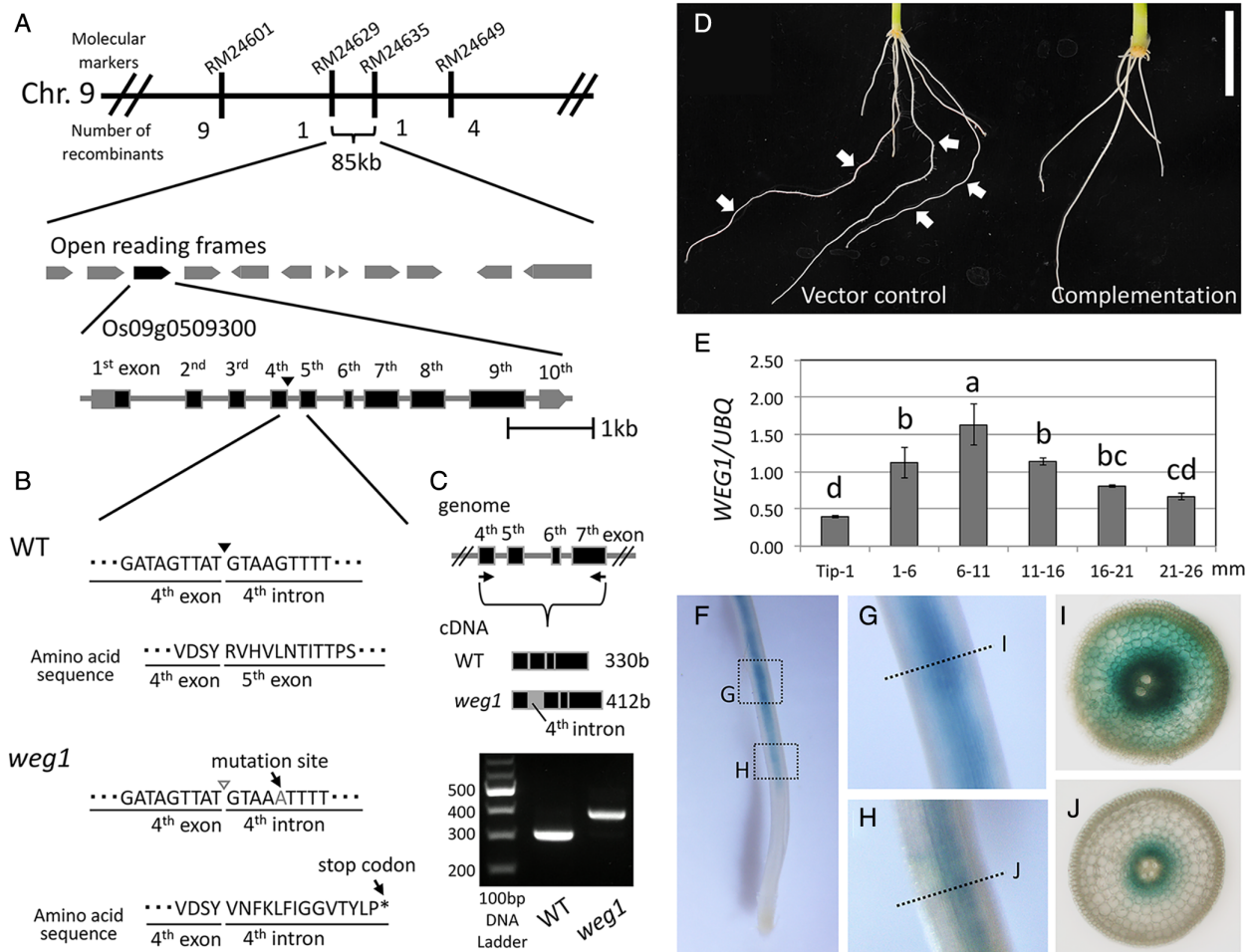


Fig. 4. Map-based cloning of *WEG1*, the root phenotypic complementation and the *WEG1* gene expression analysis. (A) High resolution linkage and physical map of the *WEG1* locus and the structure of the *WEG1* gene on chromosome 9. The vertical bars represent molecular markers and the number of recombinant plants indicated above and below the linkage map, respectively. The indicated black box underneath denotes the putative open reading frame for *WEG1* (Os09g0509300). Black boxes and horizontal lines indicate the exon and intron, respectively and the inverted triangle indicates the junction of the fourth exon and fourth intron. (B) The mutation site at the fourth intron showing a single base substitution difference between wild-type and mutant. (C) The *WEG1* region checked for the confirmation of mutant splicing by RT-PCR and sequencing. WT, wild-type. (D) Regenerated plants of *weg1* mutants with the vector (left) and *ProWEG1:WEG1* construct (right). Arrows point to the curvatures. Scale bar = 3.0 cm. (E) Relative expression of *WEG1* along the longitudinal axis of the seminal root. Values represent means \pm SD (n = 3). Different lowercase letters denote significant differences among regions ($P < 0.05$, 1-way ANOVA followed by Tukey's test for multiple comparisons). (F–J) Expression pattern of *WEG1* at the elongation zone of the seminal root. Scale bar = 0.5 cm. (G, H) Enlarge images of the two regions sampled from F. Scale bars = 200 μ m. (I, J) Cross-sections from G and H, respectively. Scale bars = 100 μ m.

Lateral root formation at the curved region of roots

The *weg1* mutant was also found to have significant reduction in the total number of LRs because of the reduced number of S-type LRs (Fig. 1G, H). We speculated that the wavy root phenotype affected the LR number. To examine this, we mimicked the curved region of the mutant root in the wild-type root by performing a rotation from the normal vertical growth direction to the horizontal axis at 90° and inducing gravistimulation of the root (Fig. 3A). We measured the number of LRs in the gravistimulated wild-type root at the bent region and its base and tip sides (Fig. 3B, C). The number of LRs was reduced specifically at the bent region (5.9) as compared to the opposite regions (base-15.9; tip- 16.1). Different from the S-type LR production at the bent region, the number of L-type LRs was

distinctly produced at the outer bent regions of the mutant (Fig. 1C, I) and gravistimulated wild-type roots (Fig. 3B).

Isolation of the causative gene and its preferential expression pattern in the root elongation zone

To map the causative gene, an F₂ population was developed by crossing the *weg1* mutant (derived from Tai-chung65, *japonica* variety) with the wild-type Kasalath (*indica* variety). Seedlings displaying the wavy phenotype among the progeny segregated in a 3:1 wild-type: mutant ratio, indicating that a single recessive gene caused the mutant phenotype. By using these seedlings, a map-based cloning approach was employed to isolate the causative gene; this revealed that the locus was located on chromosome 9, approximately 85 kb between the molecular

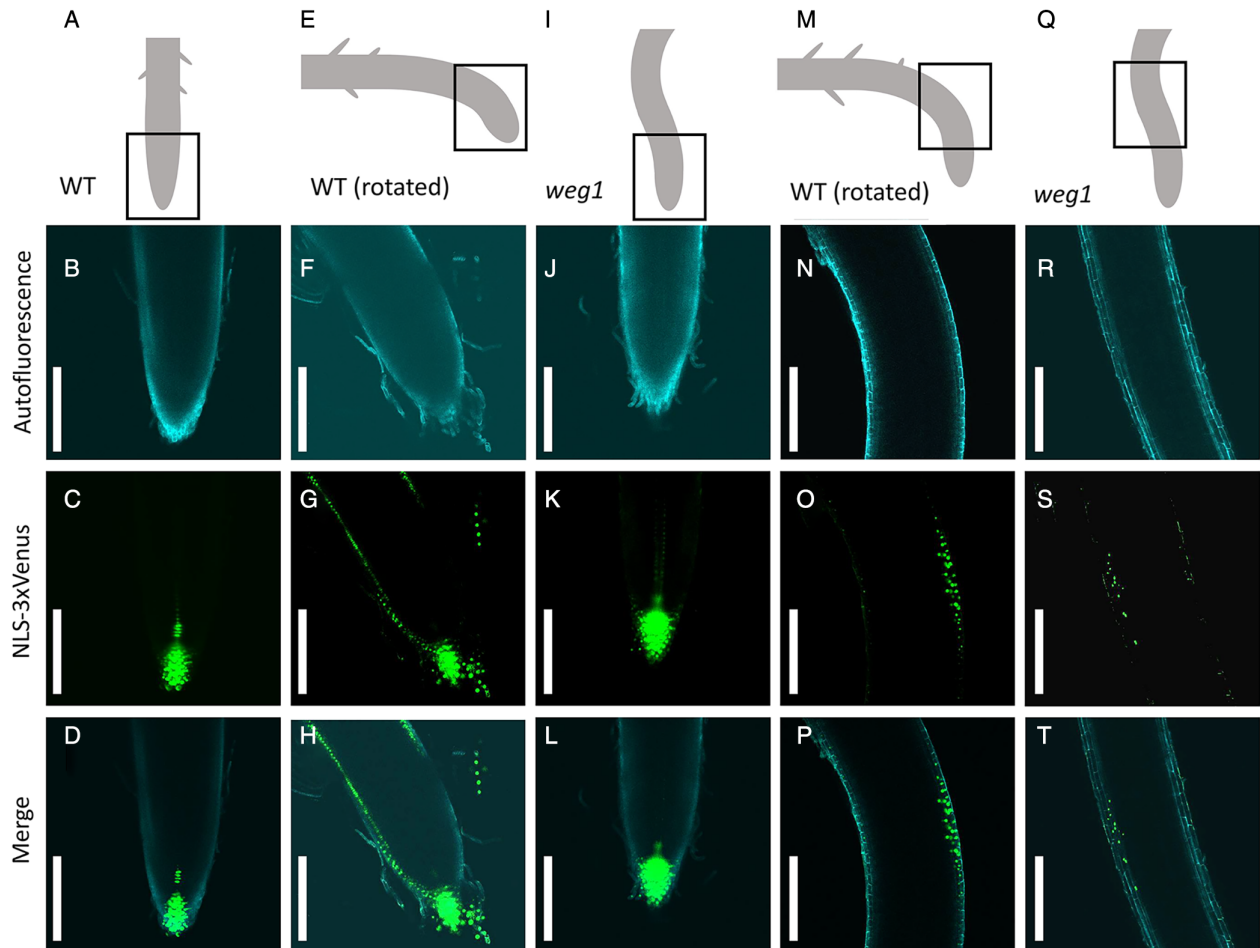


Fig. 5. Auxin distribution pattern at the root tip and curve regions in vertically-grown and gravistimulated wild-type and *weg1* mutant. (A–D) Root tip of 2-day-old wild-type grown vertically expressing *DR5:NLS-3xVenus* and (E–H) rotated from vertical to horizontal to induce gravistimulation for 4 h. (I–L) Root tip of 2-day-old *weg1* mutant expressing *DR5:NLS-3xVenus* and (M–P) the curve regions of the gravistimulated wild-type and (Q–T) *weg1* mutant. Scale bars = 200 μ m.

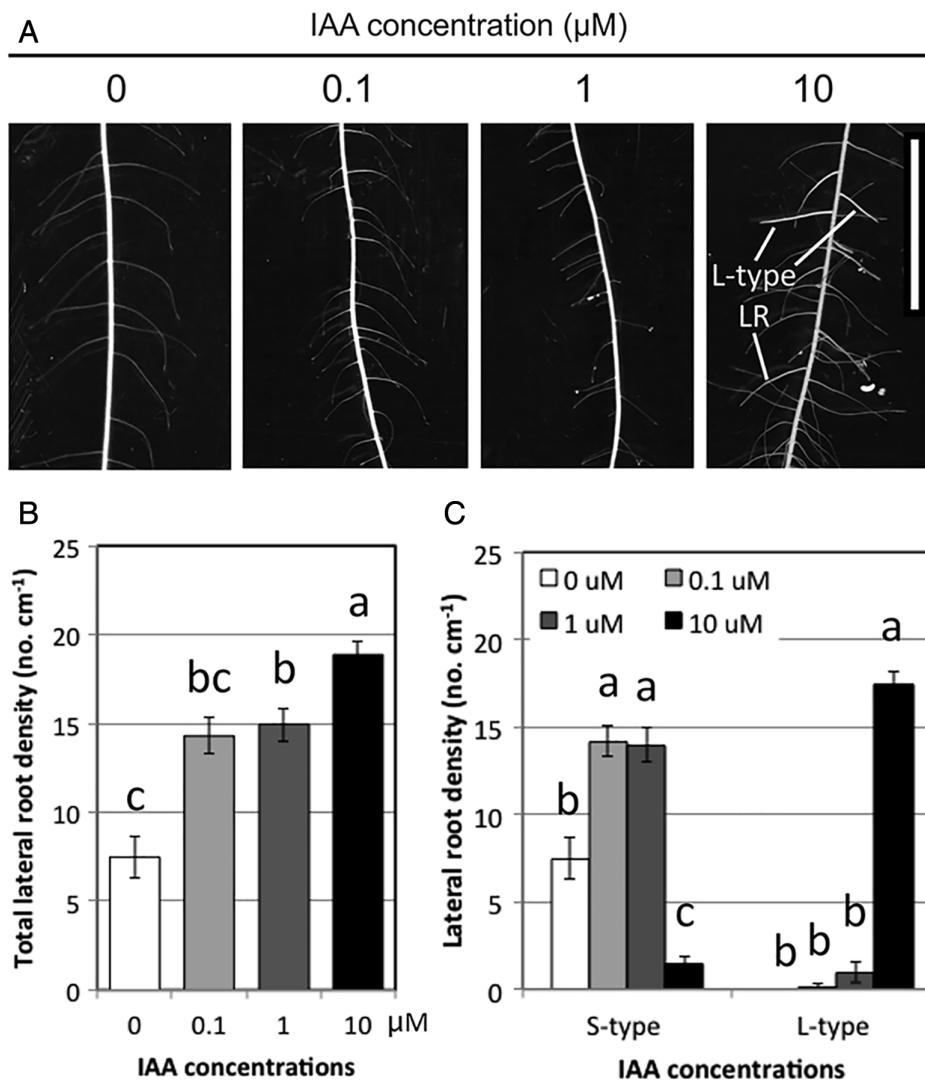


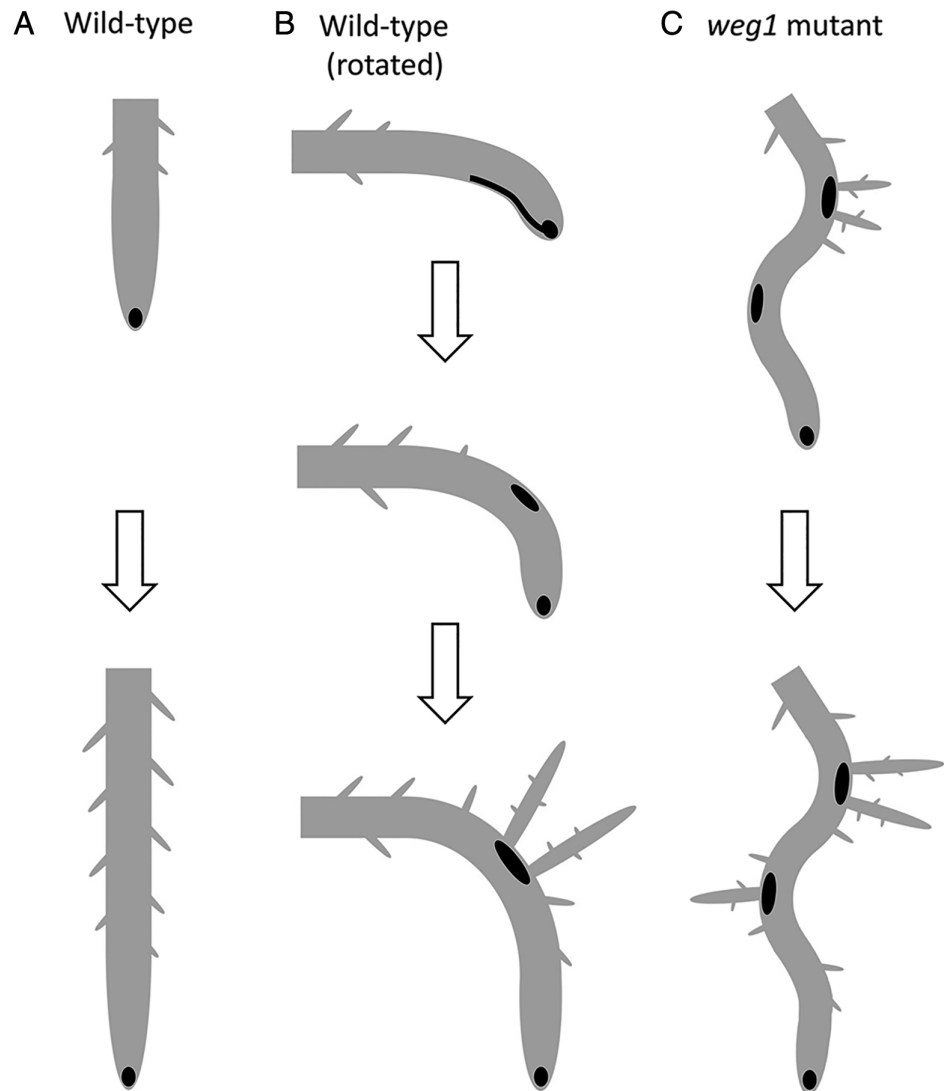
Fig. 6. Effects of auxin on lateral root development. (A) A close-up view of the lateral root development along the seminal root axis. Scale bar = 1 cm. (B) Total lateral root density and (C) S-type and L-type lateral root density at different IAA concentrations. Values represent means \pm SE ($n = 5$). Different lowercase letters denote significant differences among IAA concentrations ($P < 0.05$, 1-way ANOVA followed by Tukey's test for multiple comparisons).

markers RM24629 and RM24635 (Fig. 4A). In this region, we found a single base substitution difference in the fourth intron in Os09g0509300 between the wild-type and mutant plants, specifically at the fifth base of the fourth intron (Fig. 4B). Because this site is important for splicing, we thought that the mutant splicing was disturbed by this mutation. We then performed mRNA sequencing by synthesizing cDNA and checking the size by performing an RT-PCR using primers from the fourth and seventh exons (Fig. 4C). The size of the wild-type showed 330 bp, however, *weg1* showed a bigger size around 412 bp. Thus, we sequenced these PCR products for comparison and found that the fourth intron was not deleted, and the *weg1* amino acid sequence was changed, resulting in the generation of a stop codon, 14th amino acid after the fourth exon (Fig. 4B). Subsequently, we introduced the normal *WEG1* candidate gene under the control of its promoter (*proWEG1: WEG1*)

into the *weg1* mutant. The transformants carrying the transgene displayed the straight parental root phenotype similar to the wild-type plants (Fig. 4D). Therefore, we concluded that the *weg1* phenotype was caused by a mutation in *WEG1* (Os09g0509300).

The *WEG1* gene encodes a putative member of the HRGP family, also known as the superfamily of cell wall proteins (Showalter et al. 2010). These proteins are thought to be secreted into the cell wall where they, according to their ability, associate with and become covalently cross-linked to the cell wall components (de Cnodder et al. 2006) and are implicated in key events for plant growth and development, such as cell division and differentiation (Keller and Lamb 1989, Ito et al. 1998, Cannon et al. 2008) and cell elongation (Ito et al. 1998, de Cnodder et al. 2006). The expression pattern of *WEG1* along the longitudinal axis of the seminal root

Fig. 7. Model for auxin-dependent lateral root formation from wavy parental root. (A) Symmetric auxin accumulation in the root tip of vertically growing wild-type roots and the production of S-type lateral roots. (B) Assymmetric distribution of auxin upon gravistimulation of the wild-type roots that becomes symmetric as roots progress to grow downward. The succeeding accumulation of auxin at the bent regions alongside formation of L-type lateral roots similar to the mutant shown in C. (C) Symmetric distribution of auxin in the root tips of mutant indicating auxin-independent wavy root phenotype and the accumulation of auxin at the bent regions for L-type lateral root formation.



segmented into different zones, representing the gradient of cellular development, was analyzed using qRT-PCR. The *WEG1* transcript level was highest at the elongation zone, where cells actively elongate along the root axis, as compared to the distal end and basal zone of the root tip (Fig. 4E). We also compared the *GUS* activity under the control of the *WEG1* promoter. The *GUS* staining was observed strongly in the elongation zone (Fig. 4F). We compared the cross-sections of the elongation zone and observed that the staining was first in the stele and then largely in the cortical cells (Fig. 4G–J).

Observation of auxin distribution pattern in the apical and the curved region of roots

Gravity-induced differential root growth is caused by asymmetric redistribution of plant growth regulators,

mainly auxin, across the root. This asymmetric auxin distribution can be established when the movement of auxin to the elongation zone is higher on one side than the other (Kleine-Vehn et al. 2010, Barbez et al. 2017). To test if auxin is involved in the asymmetric root growth of the mutant, we checked the *NLS-3xVenus* expression pattern driven by the auxin response promoter *DR5* (*DR5: NLS3xVenus*) in the vertically-grown *weg1* and wild-type plants and also compared the curved region of the mutant root to the gravistimulated wild-type root. We found that the auxin signal was symmetrically confined at the root tip of the mutant (Fig. 5I–L) and it did not differ from the wild-type (Fig. 5A–D). However, the auxin signal in gravistimulated wild-type root was asymmetrically distributed, i.e., auxin was more expressed on the lower side of the bending roots than on the upper side (Fig. 5E–H). We also generated and characterized the *weg1 Osiaa13*

double mutant. The *Osiia13* mutant is defective in auxin signal transduction and, thus, shows reduced auxin sensitivity on the root tip of rice (Kitomi et al. 2012). Inahashi et al. (2018) reported that the *Ospin2* gene, which causes the wavy root phenotype caused by asymmetric auxin accumulation in root tip, was rescued by a double mutation with *Osiia13*. In contrast, the *weg1 Osiia13* double mutant still possessed the wavy root phenotype, that is, *Osiia13* did not rescue the *weg1* phenotype (Fig. 1N, O).

We also observed that auxin accumulated at the convex side of the curvatures of both *weg1* mutant and gravistimulated wild-type, with no marked differences in the auxin distribution (Fig. 5M–T). Although auxin was not involved in the wavy root elongation of *weg1*, we speculated that a high concentration of auxin is required for the development of L-type LR. Thus, we applied IAA to the wild-type seedlings grown vertically. To best see the effect of IAA, seedlings were grown in tap water condition because the wild-type produced only S-type LR in this condition (Fig. 6C) whereas it produced a small number of L-type LR under nutrient condition (Fig. 1I). We found that auxin promoted the total LR number in a dosage-dependent manner (Fig. 6A, B). Interestingly, at high auxin concentrations (10 mM IAA), the number of L-type LR was high, but that of S-type LR was low, suggesting that a high concentration of auxin is required for the formation of L-type LR (Fig. 6A, C).

Discussion

In this study, we isolated a rice mutant line, *weg1*, which exhibited a wavy parental root producing a higher number of developed L-type LR as compared to the wild-type plants, which displayed a straight parental root producing S-type LR (Fig. 1A, B, O). L-type LR are LR that are long, have a thick diameter and capable of higher order of branching while S-type LR are short, have a thin diameter and do not branch. In detailed observation, we found that these L-type LR arose from the convex side of the curvatures of the wavy parental roots of *weg1* mutant (Fig. 1C). In addition, the total LR number of *weg1* mutant seedlings was significantly reduced because of a lower S-type LR number (Fig. 1H) but other root traits, such as seminal root length and crown root number, were comparable to the wild-type seedlings (Fig. 1E, F). Previous studies have also reported mutant lines with wavy parental roots; however, they did not produce developed L-type LR along their curvatures (Wu et al. 2015, Inahashi et al. 2018). Furthermore, we observed that despite the wavy root phenotype of *weg1* mutant, the shoot length at seedling stage and the aerial parts at maturity stage, including height and panicle number, were similar to that of wild-type (Fig. 1D, J, K). These results indicate that

weg1 mutation affects only root waving and LR formation and have no retarding effects on other root components, shoot and yield, reflecting its function solely in the development of roots, thus making it suitable for the molecular studies of root development and a good material for breeding purposes.

***weg1* wavy root phenotype is determined by an asymmetric cell elongation and alters LR formation**

To understand the cellular basis of the cause of the wavy root phenotype, we performed histological analyses on the wavy root of *weg1* mutant. Actively dividing cells, indicated by EdU-covered cells, in the cell division zone of *weg1* mutant root was the same as the wild-type root (Fig. 2A, B). On the other hand, the cell lengths in the elongation zone of *weg1* mutant roots exhibited differential growth as compared to the straight growth of the wild-type roots. The cortical cell lengths of the *weg1* mutant roots at the outermost of the convex side were longer than the concave side of the bent region. These observations suggest that the wavy root phenotype is not related to cell division but is caused by the asymmetric cell elongation at the elongation zone, resulting in the formation of a curvature.

Another apparent root morphological change in *weg1* mutant was the reduced total LR number, which we speculated was caused by the wavy root phenotype (Fig. 1C, G). To investigate this, we mimicked the wavy root of *weg1* mutant to the root of wild-type by rotation and induced gravistimulation (Fig. 3A, B). The number of LR (mainly S-type LR) was specifically reduced both at the convex and concave sides of the bent region as compared to the opposite regions (base and tip) (Fig. 3C). These observations suggest that the wavy root pattern in the *weg1* mutant affected the total number of LR. Moreover, we observed that L-type LR were distinctly produced at the convex side of the bent region, suggesting that the wavy root pattern in *weg1* also affects the formation of L-type LR.

***WEG1* encodes a putative member of the HRGP family and is preferentially expressed in the root elongation zone**

The *WEG1* gene was identified as the causative gene of the *weg1* mutant (Fig. 4A–C) and encodes a putative member of the cell wall HRGP family, whose several members were reported to be involved in the regulation of cell elongation (de Cnodder et al. 2006, Showalter et al. 2010). Analysis of the expression pattern of *WEG1* along the seminal root by qRT-PCR showed that the *WEG1* transcript level was highest at the elongation zone (Fig. 4E), which coincided to the strong GUS expression pattern at the elongation zone under the *WEG1* promoter (Fig. 4F–H). Moreover, the expression pattern was largely

observed at the cortical cells (Fig. 4I, J). The localized expression pattern of the *WEG1* gene in the cortical cells at the elongation zone of the root is consistent to the wavy root phenotype of *weg1* mutant, suggesting that *WEG1* is involved in the control of cell elongation in the root.

The HRGPs are implicated in a variety of physiological processes, including embryogenesis, reproductive development and defense to biotic and abiotic stresses (Hijazi et al. 2014). In addition, they have been reported to play roles in cell expansion and growth (Cannon et al. 2008, Velasquez et al. 2011), wherein they contribute to wall assembly and remodeling to allow cell wall extension for elongation. The importance of HRGPs in polarized cell elongation were studied in the mutants that have shorter root, including *p4h13* (Velasquez et al. 2011), *lrx1* (Baumberger et al. 2003), *perk13* (Humphrey et al. 2007) and *sos5* (Shi et al. 2003) mutants, which signifies that HRGP is indispensable for normal cell elongation through cell wall modifications. As a putative member of the HRGP family, our characterization of a rice mutant defective in *WEG1* function showed that *WEG1* plays a vital role in modulating straight root growth in rice, specifically in the control of cell elongation that is probably regulated through the cell wall.

Asymmetric cell elongation causing wavy root pattern in *weg1* mutant is not linked to auxin

It is known that asymmetric auxin distribution at the elongation zone causes asymmetric cell elongation. However, we revealed that the auxin signal in the root tip of *weg1* was symmetric, similar to the wild-type grown vertically but in contrast to the gravistimulated wild-type that showed asymmetric auxin signal (Fig. 5A–L). These results suggest that auxin might not be involved in the development of the mutant wavy root phenotype. We further support this through *weg1 Osiaa13* double mutant. *Osiaa13* has a defect in auxin signal transduction resulting in the reduced auxin sensitivity of the root tip (Kitomi et al. 2012). The double mutation between *Osiaa13* and *Ospin2* (that produced wavy root pattern) resulted to the reduction of the wavy growth pattern (Inahashi et al. 2018). Unlike *Ospin2*, the *Osiaa13* did not rescue the *weg1* wavy root phenotype (Fig. 1N, O). This result may support that the asymmetric cell elongation causing wavy root phenotype of the *weg1* mutant is independent of auxin.

Auxin accumulation at the convex side of curvature is likely involved in L-type LR development

Although auxin is not likely involved in the wavy root elongation of *weg1*, we further revealed that the convex side of the curvatures of both *weg1* and gravistimulated

wild-type roots accumulated high auxin, which may suggests that high auxin concentration is required for the production of L-type LRs (Fig. 5M–T). This was supported by the exogenous IAA application to the wild-type seedlings grown vertically wherein the number of L-type LRs was high at high auxin concentrations (Fig. 6A, C), suggesting that a high concentration of auxin is required for the formation of L-type LRs.

In this study, we supposed that curvature (bending) is causal for the production of L-type LRs in rice. Moreover, auxin accumulated at the convex (outside) side of the curvature, the same area where L-type LRs occurred. This is consistent to prior reports on the observed correlations between the curvature and the site of LR formation in *Arabidopsis*, with the accumulation of auxin at the convex side of the curvature (Ditengou et al. 2008, Laskowski et al. 2008, Moreno-Risueno et al. 2010). According to Laskowski et al. (2008), the increased auxin concentrations when root bends is generated by a complex auxin flux pattern that further enhances auxin levels through localized reflux loops. The AUX1 (auxin importer) enhances the auxin maxima that specify the lateral root founder cells at the bend while PINs (efflux carriers) modulate lateral spacing of the roots along the main root axis. However, unlike *Arabidopsis* that produces one type of LR from its wavy roots, rice produces two types of LRs and we showed here the relationship between wavy parental root growth and L-type LR formation in rice. Thus, the rice plant could be used as a model to understand the mechanisms regulating the different types of LRs via auxin.

Based on our foregoing results, we propose a model for auxin-dependent LR formation (Fig. 7). Auxin accumulation is symmetrically distributed in the root tips of the vertically growing roots of the wild-type rice plants and produced S-type LRs (Fig. 7A). On the other hand, upon rotation, auxin is asymmetrically distributed in the elongation zone and then becomes symmetrically distributed in the root tip region after the root progressed to grow downward (Fig. 7B). The convex side of the bent region of the wild-type root then accumulates a high level of auxin and produces L-type LRs (Fig. 7B). In the mutant root tip region, auxin distribution is symmetric, as opposed to the asymmetric auxin distribution in the gravistimulated wild-type elongating roots, suggesting that the wavy root phenotype of the *weg1* mutant is independent of auxin. The accumulation of high auxin levels at the convex side of the curvatures of the mutant roots induced the formation of L-type LRs, similar to the bent regions of the gravistimulated wild-type roots, indicating the involvement of auxin in the formation of L-type LRs.

Conclusions

Overall, we demonstrated that the *WEG1* mutation on chromosome 9, is a single base substitution in the fourth intron of Os09g0509300 (*WEG1*), which resulted to an amino acid change, creating an early stop codon. *WEG1*, which encodes a putative member of the cell wall HRGP family, modulates straight root growth in rice, specifically in the control of cell elongation. The *weg1* mutant showed a wavy root elongation growth with highly developed L-type LRs at the convex side of the bent regions. The wavy root elongation growth is independent of auxin but the L-type LR formation is likely dependent of auxin, thus proposing a new mechanism for the regulation of these traits. Enhanced LR development would be useful for efficient water and nutrient absorption. To attain this, manipulation of the parental root pattern from straight to wavy root would be important for increasing the number of L-type LRs. In addition, the mutation has no effects on shoot growth and development despite the change in parental root growth pattern, making it a suitable material for breeding purposes. These root characteristics, therefore, might open a new breeding strategy to develop rice crops with improved root system architecture.

Author contributions

Y.I. and N.L-A. designed the study. N.L-A., T.K., M.T-N., M.K-N., C.M.W., T.H., M.H., M.S., H.Y. and Y.I. performed the experiments. N.L-A., T.K. and Y.I. analyzed the data. N.L-A., A.Y. and Y.I. wrote the manuscript with contributions from the other authors. All authors read and approved the manuscript.

Acknowledgements – We thank Dr. Kotaro Miura for providing the screening lines for rice mutants. We also thank Ms. Kimiyo Inukai, Ms. Eiko Murakami and Ms. Saki Nishiuchi for their valuable technical supports. This work was supported by PRESTO, JST, the Grant-in-Aid from the Japan Society for the Promotion of Science (No. 15H04435), the Japan Science and Technology Agency (JST)/Japan International Cooperation Agency (JICA) and the Science and Technology Research Partnership for Sustainable Development (SATREPS, No. JPMJSA1706) and JSPS KAKENHI Grant Number 18H02174.

Data availability statement

The data that support the findings of this study are available from the corresponding author upon reasonable request.

References

- Barbez E, Dünser K, Gaidora A, Lendl T, Busch W (2017) Auxin steers root cell expansion via apoplastic pH regulation in *Arabidopsis thaliana*. *Proc Natl Acad Sci U S A* 114: E4884–E4893
- Baumberger N, Steiner M, Ryser U, Keller B, Ringli C (2003) Synergistic interaction of the two paralogous *Arabidopsis* genes LRX1 and LRX2 in cell wall formation during root hair development. *Plant J* 35: 71–81
- Blancaflor E, Masson P (2003) Plant gravitropism. Unraveling the ups and downs of a complex process. *Plant Physiol* 133: 1677–1690
- Buer C, Wasteneys G, Masle J (2003) Ethylene modulates root-wave responses in *Arabidopsis*. *Plant Physiol* 132: 1085–1096
- Cannon M, Terneus K, Hall Q, Tan L, Wang Y, Wegenhart B, Chen L, Lamport D, Chen Y, Kieliszewski M (2008) Self-assembly of the plant cell wall requires an extensin scaffold. *Proc Natl Acad Sci U S A* 105: 2226–2231
- Colmer T (2003) Aerenchyma and an inducible barrier to radial oxygen loss facilitate root aeration in upland, paddy and deep-water rice (*Oryza sativa* L.). *Ann Bot* 91: 301–309
- De Cnodder T, Verbele J, Vissenberg K (2006) The control of cell size and rate of elongation in the *Arabidopsis* root. In: *The Expanding Cell*. Springer, Berlin, pp 249–269
- Ditengou F, Teale W, Kochersperger P, Flittner K, Kneupera I, van der Graaff E, Nzienguia H, Pinosaa F, Lia X, Nitschke R, Laux T, Palme K (2008) Mechanical induction of lateral root initiation in *Arabidopsis thaliana*. *Proc Natl Acad Sci U S A* 105: 18818–18823
- Fox J (2005) The R commander: a basic-statistics graphical user interface to R. *J Stat Softw* 14: 1–42
- Hiei Y, Ohta S, Komari T, Kumashiro T (1994) Efficient transformation of rice (*Oryza sativa* L.) mediated by agrobacterium and sequence analysis of the boundaries of the T-DNA. *Plant J* 6: 271–282
- Hijazi M, Velasquez S, Jamet S, Estevez J, Albenne C (2014) An update on post-translational modifications of hydroxyproline-rich glycoproteins: toward a model highlighting their contribution to plant cell wall architecture. *Front Plant Sci* 5: 1–10
- Humphrey T, Bonetta D, Goring D (2007) Sentinels at the wall: cell wall receptors and sensors. *New Phytol* 176: 7–21
- Inahashi H, Shelley J, Yamauchi T, Nishiuchi S, Takahashi-Nosaka M, Matsunami M, Ogawa A, Noda Y, Inukai Y (2018) OsPIN2, which encodes a member of the auxin efflux carrier proteins, is involved in root elongation growth and lateral root formation patterns via the regulation of auxin distribution in rice. *Physiol Plant* 164: 216–225
- IPCC (2014) Global and sectoral aspects, Climate change 2014: Impacts, adaptation, and vulnerability: Part A. Contribution of working group. In: Field CB, Barros VR,

- Dokken DJ, Mach KJ, Mastrandrea MD, Bilir TE, Chatterjee M, Ebi KL, Estrada YO, Genova RC, Girma B, Kissel ES, Levy AN, MacCracken S, Mastrandrea PR, White LL (eds) *To the Fifth Assessment Report of the Intergovernmental Panel on Climate Change*, Vol. II. Cambridge University Press, Cambridge, UK, pp 1–1132
- Ito M, Kodama H, Komamine A, Watanabe A (1998) Expression of extensin genes is dependent on the stage of the cell cycle and cell proliferation in suspension-cultured *Catharanthus roseus* cells. *Plant Mol Biol* 36: 343–351
- Kawai T, Nosaka-Takahashi M, Yamauchi A, Inukai Y (2017) Compensatory growth of lateral roots responding to excision of seminal root tip in rice. *Plant Root* 11: 48–57
- Keller B, Lamb C (1989) Specific expression of a novel cellwall hydroxyproline-rich glycoprotein gene in lateral root initiation. *Genes* 3: 1639–1646
- Kitomi Y, Inahashi H, Takehisa H, Sato Y, Inukai Y (2012) OslAA13-mediated auxin signaling is involved in lateral root initiation in rice. *Plant Sci* 190: 116–122
- Kleine-Vehn J, Ding Z, Jones AR, Tasaka M, Morita MT, Friml J (2010) Gravity-induced PIN transcytosis for polarization of auxin fluxes in gravity-sensing root cells. *Proc Natl Acad Sci U S A* 107: 22344–22349
- Kono Y, Igeta M, Yamada N (1972) Studies on the developmental physiology of the lateral roots in rice seminal roots. *Proc Crop Sci Soc Japan* 41: 192–204
- Laskowski M, Grieneisen V, Hofhuis H, Hove C, Hogeweg P, Marée A, Scheres B (2008) Root system architecture from coupling cell shape to auxin transport. *PLoS Biol* 6: e307
- Lynch JP (2007) Roots of the second green revolution. *Aust J Bot* 55: 493–512
- Masson P (1995) Root gravitropism. *Bioessays* 17: 119–127
- Mochizuki S, Harada A, Inada S, Sugimoto-Shirasu K, Stacey N, Wada T, Sishiguro S, Okada K, Sakai T (2005) The arabidopsis WAVY GROWTH 2 protein modulates root bending in response to environmental stimuli. *Plant Cell* 17: 537–547
- Moreno-Risueno M, Van Norman J, Moreno A, Zhang J, Ahnert S, Benfey P (2010) Oscillating gene expression determines competence for periodic *Arabidopsis* root branching. *Science* 329: 1306–1311
- Murashige T, Skoog F (1962) A revised method for rapid growth and bioassays with tobacco tissue cultures. *Physiol Plant* 15: 472–497
- Nakagawa T, Suzuki T, Murata S, Nakamura S, Hino T, Maeo K, Tabata R, Kawai T, Tanaka K, Niwa Y, Watanabe Y, Nakamura K, Ishiguro S (2007) Improved gateway binary vectors: high-performance vectors for creation of fusion constructs in transgenic analysis of plants. *Biosci Biotechnol Biochem* 71: 2095–2100
- Niones J, Inukai Y, Suralta R, Yamauchi A (2015) QTL associated with lateral root plasticity in response to soil moisture fluctuation stress in rice. *Plant and Soil* 391: 63–75
- Oliva M, Dunand C (2007) Waving and skewing: how gravity and the surface of growth media affect root development in *Arabidopsis*. *New Phytol* 176: 37–43
- Ozawa K (2009) Establishment of high efficiency *Agrobacterium*-mediated transformation system of rice (*Oryza sativa*). *Plant Sci* 176: 522–527
- Rebouillat J, Dievart A, Verdeil J, Escoute J, Giese G, Breitler J, Gante P, Espeout S, Guiderdoni E, Perin C (2009) Molecular genetics of rice root development. *Rice* 2: 15–34
- Satoh H, Omura T (1979) Induction of mutation by the treatment of fertilized egg cell with N-methyl-N-nitrosourea in rice. *J Fac Agric Kyushu Univ* 24: 165–174
- Shi H, Kim Y, Guo Y, Stevenson B, Zhu J (2003) The *Arabidopsis* SOS5 locus encodes a putative cell surface adhesion protein and is required for normal cell expansion. *Plant Cell* 15: 19–32
- Showalter A, Keppler B, Lichtenberg J, Gu D, Welch L (2010) A bioinformatics approach to the identification, classification and analysis of hydroxyproline-rich glycoproteins. *Plant Physiol* 153: 485–513
- Suralta R, Lucob N, Perez L, Nguyen H (2015) Developmental and quantitative trait loci analyses of root plasticity in response to soil moisture fluctuation in rice. *Philipp J Crop Sci* 40: 12–24
- Suralta R, Kano-Nakata M, Niones J, Inukai Y, Kameoka E, Tran T, Menge D, Mitsuya S, Yamauchi A (2016) Root plasticity for maintenance of productivity under abiotic stressed soil environments in rice: progress and prospects. *Field Crops Res* 220: 57–66. <https://doi.org/10.1016/j.fcr.2016.06.023>
- Uga Y, Okuno K, Yano M (2011) Dro1, a major QTL involved in deep rooting of rice under upland field conditions. *J Exp Bot* 62: 2485–2494
- Uga Y, Sugimoto K, Ogawa S, Rane J, Ishitani M, Hara N, Kitomi Y, Inukai Y, Ono K, Kanno N, Inoue H, Takehisa H, Motoyama R, Nagamura Y, Wu J, Matsumoto T, Takai T, Okuno K, Yano M (2013) Control of root system architecture by DEEPER ROOTING 1 increases rice yield under drought conditions. *Nat Genet* 45: 1097–1102
- Uga Y, Kitomi Y, Ishikawa S, Yano M (2015) Genetic improvement for root growth angle to enhance crop production. *Breed Sci* 65: 111–119
- Velasquez S, Ricardi M, Dorosz J, Fernandez P, Nadra A, Pol-Fachin L, Egelund J, Gille S, Harholt J, Ciancia M, Verli H, Pauly M, Bacic A, Olsen C, Ulvskov P, Petersen B, Somerville C, Iusem N, Estevez J (2011) O-glycosylated cell wall proteins are essential in root hair growth. *Science* 332: 1401–1403
- Wang H, Inukai Y, Kamoshita A, Wade L, Nguyen H, Yamauchi A (2005) QTL analysis on plasticity in lateral

- root development in response to water stress in rice plants. In: Toriyama K, Heong KL, Hardy B (eds) *The Proceedings of the World Rice Research Conference: Rice is Life: Scientific Perspectives for the 21st Century*, Tsukuba, Japan, pp 464–469. <http://large.stanford.edu/courses/2016/ph240/mccall1/docs/toriyama.pdf>
- Wu S, Xie Y, Zhang J, Ren Y, Zhang X, Wang J, Guo X, Wu F, Sheng P, Wang J, Wu C, Wang H, Huang S, Wan J (2015) VLN2 regulates plant architecture by affecting microfilament dynamics and polar auxin transport in rice. *Plant Cell* 27: 2829–2845
- Yamauchi A, Kono Y, Tatsumi J (1987) Comparison of root system structures of 13 species of cereals. *Jpn J Crop Sci* 56: 618–631
- Yamauchi A, Pardales J, Kono Y (1996) Root system structure and its relation to stress tolerance in: Ito O, Johansen C, Gyamfi J, Katayama K, Kumar J, Rego T (eds.), *Dynamics of Roots and Nitrogen in Cropping Systems of the Semiarid Tropics*. pp. 211–223, JIRCAS, Tsukuba, Japan

Supporting information

Additional supporting information may be found online in the Supporting Information section at the end of the article.

Table S1. Primer sequences used for the mapping, checking of cDNA size and qRT-PCR analysis.